Networked Microgrids for Service Restoration in Resilient distribution systems

Anmar Arif[1] and Zhaoyu Wang[1,*]

[1]Department of Electrical and Computer Engineering, Iowa State University, Ames, Iowa, United States.
[*]wzy@iastate.edu

Abstract: This paper presents a novel networked microgrids (MGs)-aided approach for service restoration in power distribution systems. The paper considers both dispatchable and nondispatchable DGs, and energy storage systems. The uncertainty of the customer load demands and DG outputs are modelled in a scenario-based form. A stochastic mixed-integer linear program (MILP) is formulated with the objective to maximise the served load, while satisfying the operation constraints of the distribution system and MGs. The interaction among MGs is modelled using the type 1 special ordered set (SOS1). Two approaches are developed and compared: 1) a centralised approach where all MGs are controlled by a distribution system operator, and 2) a decentralised approach where the distribution system and MGs are managed by different entities. The proposed restoration models are tested on a modified IEEE 123-bus distribution system. The results demonstrate the advantages of leveraging networked MGs to facilitate service restoration.

Nomenclature

Sets and Indices

F	Set of faulted lines
I^D/I^{CL}	Set of buses with noncontrollable/controllable loads
I^{ES}	Set of buses with energy storage
I_n^{MG}	Set of buses in MG n (DGs)
$k(i,.)$	Set of lines with bus i as the to bus
$k(.,i)$	Set of lines with bus i as the from bus
MD	Set of lines connecting MGs and distribution system
ML	Set of connection lines among MGs
n	Index for MGs
i	Index for bus
k	Index for lines

t	Index for time

Parameters

$P_{i,t}^{D}$	Active demand at bus i
$P_{i,t}^{PV}$	Active power output of the PVs
P_{n}^{th}	Threshold active power of MG n
P_{n}^{max}/D_{n}^{max}	Maximum active power/demand in MG n
$Q_{i,t,s}^{PV}$	Reactive power output of the PVs for scenario s
w_i	Priority index of the load at bus i
η_c/η_d	Charging/discharging efficiency of the ES
ϵ	Small number
Δt	Time Step

Variables

$P_{i,t}^{CL}$	Active demand served for the controllable load at bus i
$P_{i,t}^{DG}$	Active power output of a DG
$P_{k,t,s}^{L}$	Active power flow on line k for scenario s
$P_{i,t}^{ch}/P_{i,t}^{dch}$	Charging and discharging of the ES
$Q_{i,t}^{CL}$	Reactive demand served for the controllable load at bus i
$Q_{i,t}^{DG}$	Reactive power output of a DG
$Q_{k,t,s}^{L}$	Reactive power flow on line k for scenario s
$y_{i,t}$	Connecting status of the load at bus i
$SOC_{i,t}$	State of charge of the ES
$u_{k,t}$	Switch on/off status of line k
$V_{i,t,s}$	Bus voltage magnitude at bus i for scenario s
$\varphi_{i,t}$	Charging/discharging state of the ES
$\mu_{n,t}$	Binary decision variable of MG n for exchanging power
$\Delta_{n,t,s}$	Difference between total generation and demand in a microgrid for scenario s
δ_n	Binary variable of SOS1 to determine μ_n

1. Introduction

Severe weather events such as storms, hurricanes and floods result in serious power outages. Studies show that 58% of power outages in the United States are due to severe weather, and the annual economic costs of these outages are estimated to be $\$20$ billion to $\$55$ billion [1]. For example, Hurricane Sandy left approximately 7.5 million customers without electricity and resulted in an economic loss between $\$27$ billion and $\$52$ billion [2]. It has been shown that power distribution systems are more vulnerable to extreme weather events [3]. Therefore, the power industry has been focusing on developing methods to enhance grid resilience. Power system resilience can be defined as the ability to prepare for, adapt to, and recover rapidly from disruptions caused by extreme events such as climatic hazards [4]. To improve the grid resilience, new service restoration techniques are needed to reduce the outage time and protect critical loads.

The integration of distributed generators (DGs) and microgrids (MGs) in modern distribution systems provides new opportunities to maintain the power supply to critical facilities and enable faster restoration. A MG is a localised cluster of power sources and loads that can operate in two different modes: the islanded mode and the grid-connected mode [5]. The ability to maintain self-sufficiency is a critical feature of MGs, which makes MGs suitable to be used to mitigate grid disturbances and facilitate faster system recovery during severe outages [6]. Connecting multiple MGs to be a system of networked MGs can further improve the power grid reliability and resilience [7, 8]. Networked MGs can exchange power to maintain continuous power supply within MGs during outages. Moreover, the surplus power generation of networked MGs can be used to pick up loads in the upstream distribution systems to reduce the restoration time.

The research on leveraging MGs to improve distribution system restoration is gaining increasing interests [9, 10]. The authors in [11] investigated the self-healing capability of a power distribution system by sectionalising the system into multiple MGs. In [9], black-start restoration sequences were simulated for MGs with the purpose of ensuring system stability, robustness and power quality during service restoration. Reference [12] proposed a multi-criteria decision making method to connect multiple MGs in order to exchange power. The authors in [13] presented a graph-theoretic distribution system restoration strategy incorporating MGs that maximised the restored load and minimises the number of switching operations. Although the above papers have taken advantage of networked MGs in service restoration, the optimal coordination of MGs in providing such support is not fully studied, and few papers included uncertainty and reconfiguration of the network.

In this paper, we leverage networked MGs to facilitate the service restoration while considering the uncertainty of the loads and DGs. A novel approach is proposed to dispatch the DGs and controllable loads (CLs), coordinate the power exchange among MGs, and reconfigure the network to maximise the served loads. Two approaches are developed and compared. The first is a centralised approach where all MGs, line switches, and controllable loads are managed by the distribution system operator to optimise the served loads in the entire system. In the first approach, MGs act selflessly for the goodness of the whole system. The second approach is a decentralised approach where the distribution system and MGs are controlled by different entities with their own objectives. Each MG operates its own network and decides whether to connect to the distribution system or not. In this case, the MGs act selfishly and the computation burden is reduced. Each MG decides to support other MGs based on its generation-demand balance. Two MGs are connected only if both MGs decide to exchange power. A linear decision-making function is developed to model the coordinated power exchange among MGs. The linear decision-making process is represented by a mixed integer linear programming (MILP) problem with the type 1 special ordered

set (SOS1) [14]. SOS1 is a set that contains non-negative variables, of which only one can take a strictly positive value, all others are zeros. Multiple types of DGs are taken into account in this paper, which include Micro Turbines (MT), Photovoltaic (PV) generators, and electric storage devices (ES). The uncertainty of DG outputs and customer demands are considered in a scenario-based form. The model is tested on a modified IEEE 123-bus distribution system with multiple outages.

The rest of the paper is organised as follows. Modelling uncertainty and scenario generation are presented in Section II. Section III presents the formulation of the developed model and introduces the centralised and decentralised approaches. Section IV presents the simulation results. Finally, Section V concludes the paper.

2. Modelling Uncertainty

In this paper, the PVs are considered as nondispatchable DGs. The power generated by PVs is dependent on the incident solar irradiance level, while the irradiance depends on the cloud coverage level (CCL). The sky condition can be divide to four categories: clear, partly clear, mostly cloudy, and overcast. It is assumed that the sky condition is clear in the test case presented in this paper. CCL is determined randomly as defined in Table 1 [15].

Table 1 Cloud Coverage Level Probability

CCL	Probability of occurrence
0.00 - 0.05	0.67
0.05 - 0.15	0.19
0.15 - 0.25	0.14

Monte Carlo simulation is used to generate a finite set of random scenarios representing the forecasted power uncertainty. This uncertainty is modelled through CCL in each time period. Therefore, the cloud coverage level can be represented as $CCL(t, s)$, where t is the hour of the day and s is the scenario. The random values of CCL are used to calculate the current solar irradiance level using (1).

$$Irr(t, s) = Irr^{max}(t) \cdot [1 - CCL(t, s)] \tag{1}$$

where $Irr(t, s)$ is the solar irradiance level at time t and scenario s, and $Irr^{max}(t)$ is the maximum irradiance at instant t. An example of a generated scenario is given in Fig. 1. For a PV cell rated at P^{PV}_{max}, it can produce that amount when the solar irradiance is 1000 $\mathrm{W/m^2}$. The output power of the PVs can be calculated using (2).

$$P^{PV}_{i,t,s} = \frac{Irr(t, s)}{1000\mathrm{W/m^2}} P^{PV}_{max} \tag{2}$$

As for load uncertainty, it is modelled using load forecasting error [16]. Let $P^F_{i,t}$ be the load forecast for load at bus i at time t, and $e_{i,s}$ is the load forecasting error for scenario s. The random variable $e_{i,s}$ is generated using a truncated normal distribution model, so that the error is within 15% of the forecasted value. The active demand is determined by (3), and the same equation is used for the reactive demand.

$$P^D_{i,t,s} = P^F_{i,t}(1 + e_{i,s}) \tag{3}$$

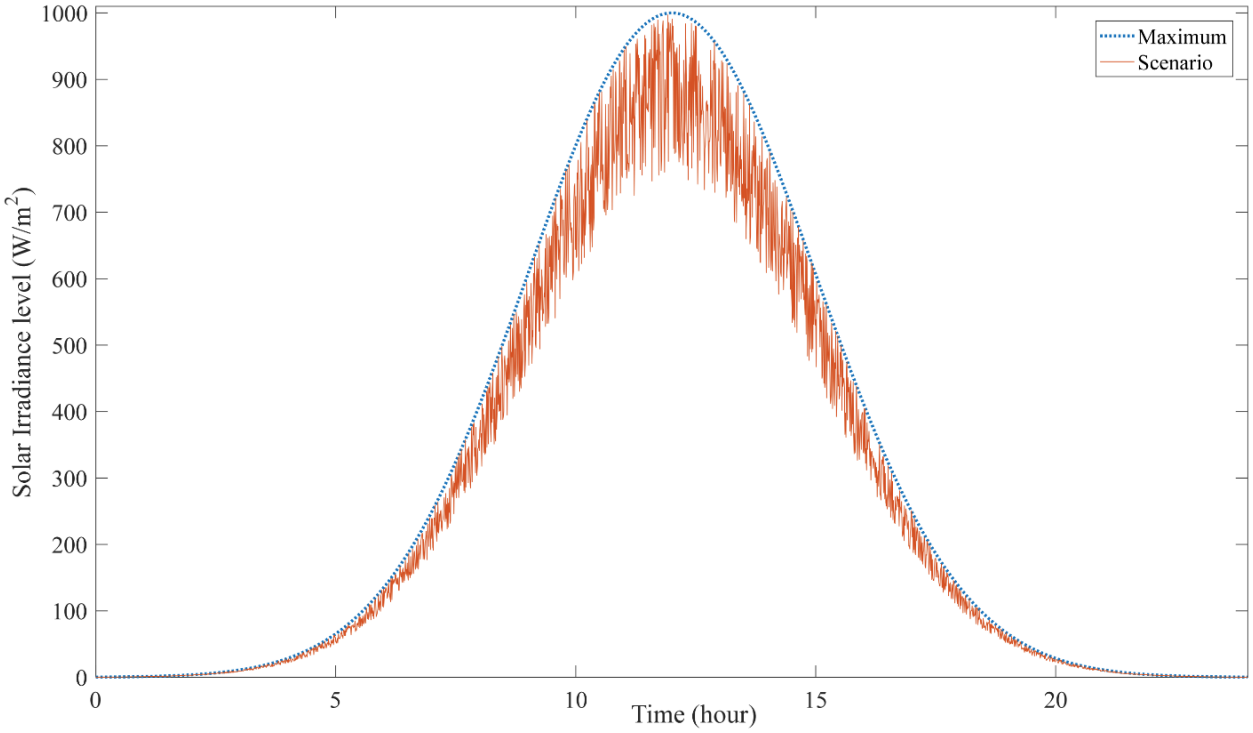

Fig. 1. *A scenario example for the solar irradiance level prediction*

3. Mathematical Formulation

This section presents the detailed mathematical formulation for the MG-aided restoration problem. The formulation includes the distribution system, energy storage system (ESS), and MG power exchange models.

3.1. Objective

$$\zeta = \max \sum_{\forall s} \Pr(s) \left(\sum_{\forall t} \left(\sum_{\forall i \in I^D} y_{i,t}\, w_i\, P^D_{i,t,s} + \sum_{\forall i \in I^{CL}} P^{CL}_{i,t} \right) \right) \tag{4}$$

After outages, the main objective of the restoration is to maximise the served loads. The objective function (4) is the summation of the active power of non-controllable loads P^D and controllable loads P^{CL}. A priority factor w_i is assigned to each load. The binary variable $y_{i,t}$ indicates whether a load is being supplied ($y_{i,t}$ = 1) or not ($y_{i,t}$ = 0).

$$0 \le P^{CL}_{i,t} \le P^{CL}_{max} \quad \forall i \in I^{CL}, t \tag{5}$$

$$0 \le Q^{CL}_{i,t} \le Q^{CL}_{max} \quad \forall i \in I^{CL}, t \tag{6}$$

$$y_{i,t+1} \ge y_{i,t}\ , \ \forall i, t \tag{7}$$

Constraints (5) and (6) guarantee that the restored controllable load consumption is within a certain range. Once a load is served, it should remain energized, which is enforced by (7).

3.2. Distribution System Power Flow

The most commonly used power flow model is the linear DC optimal power flow model, but the model neglects reactive power and voltage levels. On the other hand, AC optimal power-flow is nonlinear and will increase the computational complexity. Therefore, linearized DistFlow equations are used to calculate the active and reactive power flow, and the voltages at each bus. Linearized Distflow equations have been used and verified in the literature for traditional distribution systems and MGs [7, 17, 18]. The power flow equations are formulated as follows:

$$\sum_{\forall k(i,.)} P^{L}_{k,t,s} - \sum_{\forall k(.,i)} P^{L}_{k,t,s} + P^{DG}_{i,t,s} + P^{dch}_{i,t} - P^{ch}_{i,t} + P^{PV}_{i,t,s} - y_{i,t} P^{D}_{i,t,s} - P^{CL}_{i,t} = 0,\ \forall i,t,s \quad (8)$$

$$\sum_{\forall k(i,.)} Q^{L}_{k,t,s} - \sum_{\forall k(.,i)} Q^{L}_{k,t,s} + Q^{DG}_{i,t,s} + Q^{PV}_{i,t,s} - y_{i,t} Q^{D}_{i,t,s} - Q^{CL}_{i,t} = 0,\ \forall i,t,s \quad (9)$$

$$-(1-u_{k,t})M \ \leq V_{j,t,s} - V_{i,t,s} + \frac{R_k P^{L}_{k,t,s} + X_k Q^{L}_{k,t,s}}{V_1} \ \leq (1-u_{k,t})M,\ \forall k,t,s \quad (10)$$

$$1-\epsilon \leq V_{i,t,s} \leq 1+\epsilon\ ,\ \forall i,t,s \quad (11)$$

$$0 \leq P^{DG}_{i,t,s} \leq P^{DGmax}_{i}\ ,\ \forall i,t,s \quad (12)$$

$$0 \leq Q^{DG}_{i,t,s} \leq Q^{DGmax}_{i}\ ,\ \forall i,t,s \quad (13)$$

$$-u_{k,t} P^{Lmax}_{k} \leq P^{L}_{k,t,s} \leq u_{k,t} P^{Lmax}_{k}\ ,\ \forall k,t,s \quad (14)$$

$$-u_{k,t} Q^{Lmax}_{k} \leq Q^{L}_{k,t,s} \leq u_{k,t} Q^{Lmax}_{k}\ ,\ \forall k,t,s \quad (15)$$

Constraints (8) and (9) represent the active and reactive power balance constraints respectively. P^{DG} is the power supplied by the dispatchable DGs, while P^{ch}/P^{dch} are the charging and discharging power for the ESS. The voltage at each bus is expressed in constraint (10), where V_1 is the reference voltage. A *big M* method is used to ensure that the voltage levels of two disconnected buses are decoupled. The status of a line with a switch is determined by binary variable u, which equals 1 if it is ON and zero for OFF. Constraint (11) defines the allowable range of voltage deviations, where ϵ is set to be 5%. Constraints (12) and (13) define the output limits for dispatchable DGs, respectively. The line limits are defined in (14) and (15), which indicate that the power flow through a switch should be zero if it is OFF. The automatic switches are controlled by $u_{k,t}, k \in SW$ to reconfigure the network. The switching status of a line $u_{k,t}$ is set to be 1 when there is no fault and/or no switch in (16).

$$u_{k,t} = 1, \forall k \notin \{SW \cup F\}, t \quad (16)$$

3.3. Energy Storage System

$$SOC^{min}_{i} \leq SOC_{i,t} \leq SOC^{max}_{i}\ \forall i \in I^{ES}, t \quad (17)$$

$$SOC_{i,t} = SOC_{i,t-1} + \Delta t\ \left(\eta_c P^{ch}_{i,t} - \eta_d^{-1} P^{dch}_{i,t}\right)\ \forall i \in I^{ES}, t \quad (18)$$

$$0 \leq P^{ch}_{i,t} \leq P^{ch,max}_{i} \varphi_{i,t}\ \forall i \in I^{ES}, t \quad (19)$$

$$0 \leq P^{dch}_{i,t} \leq P^{dch,max}_{i} (1-\varphi_{i,t})\ \forall i \in I^{ES}, t \quad (20)$$

The operation of ESS is modelled in constraints (17)-(20). Constraint (17) represents the minimum and maximum levels of state of charge (SOC) of an ESS, which are assumed to be 20% and 90% of its capacity, respectively. Constraint (18) calculates the SOC of the ES. η denotes the efficiency of the charging/discharging, which is assumed to be 0.95, and Δt is the time step. The initial state is set to be the maximum SOC. The power limits of charging/discharging are imposed in constraints (19) and (20) [19].

3.4. Reconfiguration

Unlike transmission networks, which are often meshed networks, distribution systems are commonly operated in a radial topology. Radial networks include automatic switches for reconfiguring the network in case of faults or maintainance. The distribution system is reconfigured dynamically using switches but must maintain its radial configuration. The radiality constraints are represented by (21)-(24) based on the spanning tree approach in [20].

$$0 \leq \beta_{i,j,t} \leq 1, \forall i, j, t \tag{21}$$

$$\beta_{i,j,t} + \beta_{j,i,t} = u_{k,t}, \ \forall k, t \tag{22}$$

$$\beta_{i,j,t} = 0, \ \forall i, j \in I^{SB}, t \tag{23}$$

$$\sum_{\forall i} \beta_{i,j,t} \leq 1, \ \forall j, t \tag{24}$$

$$v_{k,t} \geq u_{k,t} - u_{k,t-1}, \forall k, t \tag{25}$$

$$v_{k,t} \geq u_{k,t-1} - u_{k,t}, \forall k, t \tag{26}$$

$$\sum_{\forall t} v_{k,t} \leq N_{SW}, \forall k \tag{27}$$

$\beta_{i,j,t}$ and $\beta_{j,i,t}$ are defined to model the spanning tree (21). $\beta_{i,j,t}$ equals 1 if bus i is the parent bus to child bus j. Each bus is connected to one parent bus in a radial network, other than the root bus. Constraint (22) presents the relation between the connection status of the line and the spanning tree variables $\beta_{i,j,t}$ and $\beta_{j,i,t}$. If the distribution line is connected, then $\beta_{i,j,t}$ or $\beta_{j,i,t}$ must be one. Constraint (23) designates the substation as a root bus. Constraints (24) requires that every bus has at most one parent bus. Binary variable v is introduced to limit the number of switching. Constraints (25) and (26) sets $v_{k,t}$ to $\max\{u_{k,t} - u_{k,t-1}, u_{k,t-1} - u_{k,t}\}$. The number of switching is limited (N_{SW}) as frequent switching can cause stability issues and is impractical in real-time operation. The switching is limited by using (27).

3.5. MG Power Exchange

$$\Delta_{n,t} = \sum_{\forall i \in I_n^{MG}} (P_i^{DGmax} + P_{i,t}^{dch} + P_{i,t}^{PV_F} - P_{i,t}^{ch}) - \sum_{\forall i \in I_n^{MG}} \left(y_{i,t} P_{i,t}^{F} + P_{i,t}^{CL}\right) \ \forall n, t, s \tag{28}$$

$$- D_n^{max} \delta_{\mathrm{n},t}^{A} - \epsilon \delta_{n,t}^{B} + (P_n^{th} + \epsilon) \delta_{n,t}^{C} \leq \Delta_{n,t} \ \forall n, t, s \tag{29}$$

$$\Delta_{n,t} \leq \ - \epsilon \delta_{n,t}^{A} + (P_n^{th} + \epsilon) \delta_{n,t}^{B} + P_n^{max} \delta_{n,t}^{C} \ \forall n, t, s \tag{30}$$

$$\delta_{n,t}^{A} + \delta_{n,t}^{B} + \delta_{n,t}^{C} = 1 \ \forall n, t \tag{31}$$

$$\mu_{n,t} = \delta_{n,t}^{A} + \delta_{n,t}^{C} \ \forall n, t \tag{32}$$

$$u_{k,t} \leq \mu_{n,t}, \quad \forall k \in MD, \ \forall t \tag{33}$$

$$2u_{k,t} \leq \mu_{n,t} + \mu_{m,t}, \quad \forall k \in ML, \ \forall t \tag{34}$$

Each MG makes a decision on whether to connect to other MGs and/or the upstream distribution system based on its forecasted generation-demand balance. The difference between the total generation and demand within MG n is denoted by $\Delta_{n,t}$, which is defined in constraint (28). $P_{i,t}^{PV_f}$ is the forecasted PV output, which is assumed to be at CCL = 0. The decision on whether to exchange energy or not is denoted by binary variable $\mu_{n,t}$, which is defined in (35).

$$\mu_{n,t} = \begin{cases} 0\ , \ 0 \leq \Delta_{n,t} \leq P_n^{th} \\ 1\ , \quad o.w. \end{cases} \qquad \forall n, t, s \tag{35}$$

Equation (35) is demonstrated in Fig. 2. If the generated power in a MG is larger than the total demand within the MG by a threshold value P_n^{th}, the MG exchanges power to support the distribution system and/or other MGs upon their requests. A small value ϵ is used to account for rounding errors. The conditional constraint (35) is modelled as a mixed integer linear model in

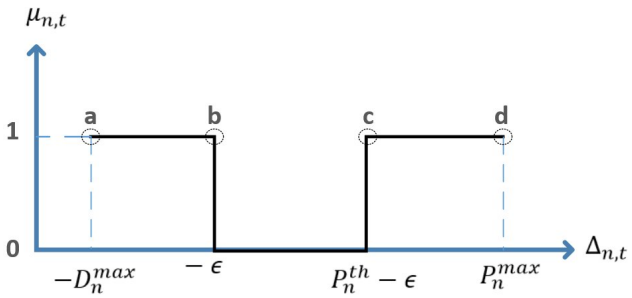

Fig. 2. *Conditional constraint* $\mu_{n,t}$

constraints (29)-(32) using SOS1. P_n^{max} and -D_n^{max} represent the maximum total generated power and maximum total demand in a MG, respectively. SOS1 introduces three binary variables denoted as $\delta_{n,t}^A$,$\delta_{n,t}^B$ and $\delta_{n,t}^C$. In constraint (29), the values of $\Delta_{n,t,s}$ at the first three points (a, b, c) are multiplied by the binary variables to set the lower bound for $\Delta_{n,t,s}$. The upper bound is set by taking the last three points (b, c, d) as shown in constraint (30). Only one binary variable can be "1" as enforced by constraint (31). Finally, the three levels (1, 0, 1) in Fig. 2 are multiplied by the binary variables; i.e., $1\ \delta_{n,t}^A + 0\ \delta_{n,t}^B + 1\ \delta_{n,t}^C$, which gives constraint (32). For illustration, if $\Delta_n = 1 (< P_n^{th})$, then $\delta_{n,t}^B = 1$, $\delta_{n,t}^A$ and $\delta_{n,t}^C$. Hence, $-\epsilon \leq \Delta_n \leq P_n^{th} - \epsilon$ and $\mu_n = 0$, which is the expected response as the MG does not have extra power to exchange. If $\delta_{n,t}^C = 0$, then this would lead to invalid boundaries. For the line connecting MG n and MG m, its switch ON/OFF status is decided by:

$$u_{k,t} \leq \mu_{n,t}\mu_{m,t} = \begin{cases} 1\ , \ \mu_{n,t} = 1, \ \mu_{m,t} = 1 \\ 0\ , \quad o.w. \end{cases} \quad \forall k \in ML, t \tag{36}$$

This equation is represented by a linear equation in constraint (34). Similarly, constraint (33) represents the decisions of MGs to exchange power with the upstream distribution system. Fig. 3 illustrates the operation of networked MGs.

3.6. Stochastic MILP

The proposed model is formulated as:

$$\zeta = \max\{(4) \mid \text{s.t. } (5) - (34), (\delta, u, \mu, v, y, \varphi) \in \{0, 1\}\} \tag{37}$$

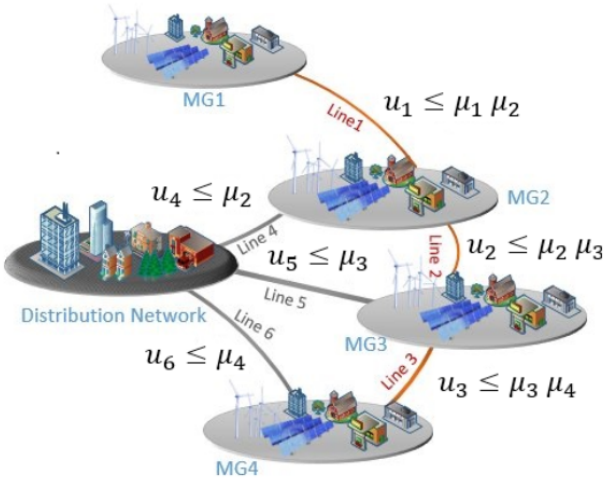

Fig. 3. *Energy exchange among microgrids*

The stochastic MILP has two-stages which are solved at the same time in (37) [21]. The first-stage includes the operation of the switches and load shedding, while the second-stage depends on the uncertainty of the PVs and load forecast. The stochastic model is implemented using the PySP package in Pyomo and solved using the extensive form with CPLEX 12.6 (http://www.pyomo.org).

3.7. Centralised and Decentralised Operations

Two operation methods are considered in this paper: centralised and decentralised ones [22–24]. In the centrelised operation, (37) is solved directly, i.e., the system including MGs are treated as a single entity. Alternatively, the decentrilised operation considers each MG as an independent entity with its own objective. Therefore, each MG solves its own power-flow problem and decides whether to interconnect with the rest of the system based on the generation-load balance. The decentrlised operation is formulated as follows:

Decentralised Operation

1. For each microgrid n, compute:
$\mu_{n,t} = \text{argmax}\{(4) \mid \text{s.t. } (5)-(32)\}$
If $\exists(i,t) : y_{i,t} = 0$ **then**: set $\mu_{n,t} = 1$
2. Compute:
$\zeta = \max\{(4) \mid \text{s.t. } (5)-(27),(33)-(34)\}$

4. Simulation and Results

As shown in Fig. 4, a modified IEEE 123-bus distribution system is used as a test case for the stochastic MG-aided restoration problem. The distribution system has four microgrids and three lines are assumed to be damaged at 10:00 AM. It is assumed that the lines are repaired after five hours. The network contains seven 250 kW MTs, six 80 kW PVs, four 100 kW batteries, and five controllable loads. The initial SOC is set to be at 90%. Loads are classified into two cataegories: regular loads and critical loads. The problem is modelled on a time step of 1 hour. Detailed information on the network can be found in [25]. The Monte Carlo sampling technique is used to generate 30 random scenarios with equal probability. The scenarios are generated using the

methods presented in Section 2. Samples of the 30 generated scenarios is shown in Fig. 5 for the active power forecast of a single load. An example of a generated scenario for the PVs was given in Fig. 1.

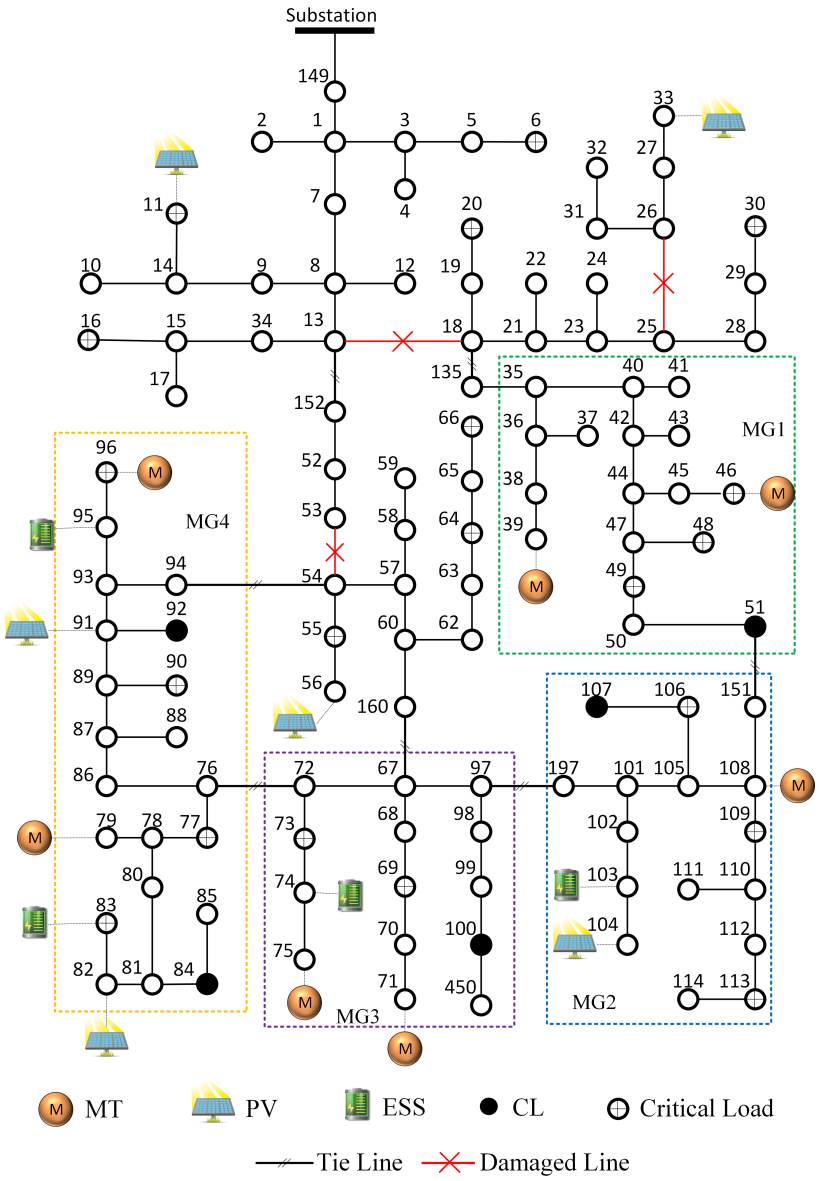

Fig. 4. *Modified IEEE 123-bus distribution system, test case*

The simulation is performed on Iowa State University's Condo cluster, whose individual blades consist of two 2.6 GHz 8-Core Intel E5-2640 v3 processors and 128GB of RAM. A comparison between the two proposed methods is shown in Table 2. The objective value ζ is found to be higher for the centralised approach, while the decentralised approach require less computation time.

In the centralised approach, 6 loads are shed within MGs and 4 loads outside, all are low-priority loads. The MGs shed few of their low-priority loads in order to provide energy to the loads in the distribution system. This allows the MGs to have surplus power to exchange with the rest of the system. The connection status of the automatic switches is shown in Table 3. Line 72-76 is OFF to maintain radial topology. The PVs can supply a large number of loads during the first four hours,

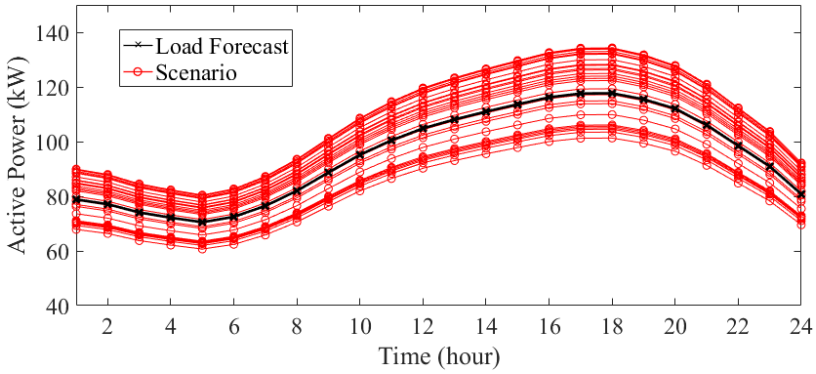

Fig. 5. *Scenarios for the active power forecast of a load*

Table 2 Comparison between the centralised and decentralised approaches

		Centralised Approach	Decentralised Approach
Objective		18845.21	18366.7516
Solution Time		324.43 s	146.23 s
Load Shed (Bus Number)	MG 1	38, 45	NA
	MG 2	111	NA
	MG 3	68, 70	68
	MG 4	86	NA
	DN	19, 31, 32, 60	19, 20, 22, 24, 28-32, 60

but the supply becomes limited as the solar irradiance decreases. Therefore, most of the energy storage devices only supply loads in the last two hours, as shown in Table 4. The active power demand served for the controllable loads is shown in Fig. 6. The MGs control the CLs by reducing their demand around peak hours.

Table 3 Connection status of the automatic switches for the centralised approach

Time	Connection status						
	13-152	18-135	51-151	54-94	67-160	72-76	97-197
10:00 AM	1	1	1	1	1	0	1
11:00 AM	1	1	1	1	1	0	1
12:00 PM	1	1	1	1	1	0	1
1:00 PM	1	1	1	1	1	0	1
2:00 PM	1	1	1	1	1	0	1
3:00 PM	1	1	1	1	1	0	1
4:00 PM	1	1	1	1	1	0	1
5:00 PM	1	1	1	1	1	0	1

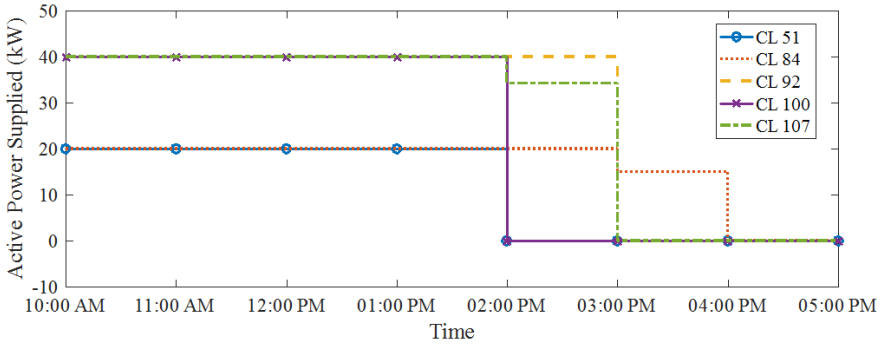

Fig. 6. *Active power supplied to the controllable loads, centrelised*

Table 4 Dispatch results of the ESSs for the centrelised approach

Time	Active Power (kW)			
	ES 74	ES 83	ES 95	ES 103
10:00 AM	0.00	0.00	0.00	20.87
11:00 AM	0.00	0.00	0.00	0.00
12:00 PM	0.00	0.00	0.00	-23.12
1:00 PM	0.00	0.00	0.00	0.00
2:00 PM	0.00	0.00	0.00	0.00
3:00 PM	0.00	0.00	0.00	0.00
4:00 PM	16.50	16.50	46.96	16.50
5:00 PM	50.00	50.00	19.54	50.00

As for the decentralized approach, MG 1 and MG 2 do not have surplus power to exchange with the other MGs and the distribution system. Therefore, lines 18-135, 51-151, and 97-197 are switched OFF as shown in Table 5. Critical loads at buses 20 and 30 are shed as MG 1 is islanded. Line 72-76 is disconnected to insure radial topology. The power supplied by the ESSs is similar to the centralized approach as shown in Table 6, but ESS 103 does not supply any power since MG 2 is not connected with MG 1 nor MG 3. The active power supplied to the CLs is shown in Fig. 7. The demand supplied to CL 51 is at its maximum value for the first six hours, in the last hour the power supplied decreases due to the increase of demand for the other loads. As observed in the centralised approach, the CLs shift their demand to off-peak hours and then decrease the demand on peak hours.

Table 5 Connection status of the automatic switches for the decentralised approach

Time	Connection status						
	13-152	18-135	51-151	54-94	67-160	72-76	97-197
10:00 AM	1	0	0	1	1	0	0
11:00 AM	1	0	0	1	1	0	0
12:00 PM	1	0	0	1	1	0	0
1:00 PM	1	0	0	1	1	0	0
2:00 PM	1	0	0	1	1	0	0
3:00 PM	1	0	0	1	1	0	0
4:00 PM	1	0	0	1	1	0	0
5:00 PM	1	0	0	1	1	0	0

Table 6 Dispatch results of the ESSs for the decentralised approach

Time	Active Power (kW)			
	ES 74	ES 83	ES 95	ES 103
10:00 AM	0.00	0.00	0.00	0.00
11:00 AM	0.00	0.00	0.00	0.00
12:00 PM	0.00	0.00	0.00	0.00
1:00 PM	0.00	0.00	0.00	0.00
2:00 PM	0.00	0.00	0.00	0.00
3:00 PM	0.00	0.00	0.00	0.00
4:00 PM	16.50	16.50	40.86	16.50
5:00 PM	50.00	50.00	25.64	50.00

It can be seen that the centralised approach produces a better overall solution. In the decentralised approach, MGs act selfishly which results in a less coordinated scheme. On the other hand, the centralised approach advocates better cooperation between MGs and the distribution system.

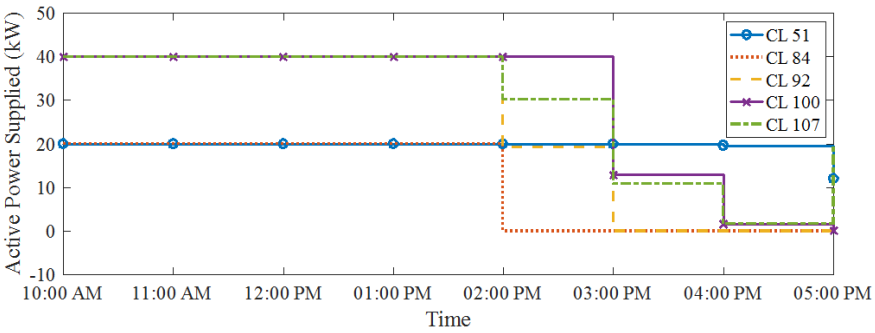

Fig. 7. *Active power supplied to the controllable loads, decentralised*

5. Conclusion

In this paper, a coordinated power exchanged mechanism for networked MGs to restore power distribution systems with outages is proposed. The MGs optimally dispatch their DG outputs in order to pick up on-outage customers. Uncertainty of the demand and PV generation is considered using Monte Carlo simulation. A linear decision-making function is employed to model each MG's capability to exchange energy. A stochastic mixed integer linear program is formulated to maximise the total loads being restored, while satisfying operation constraints. The stochastic model is solved using two approaches, centralised and decentralised ones. The proposed methods are tested on a modified IEEE 123-bus distribution system. The capabilities of networked MGs in maintaining continuous power supply and assisting system restoration are tested and validated. The results show that the interactions among MGs play an important role in facilitating the system restoration. The centralised approach emphasizes the cooperation of the MGs and the distribution to obtain a better overall result. The results confirm that the proposed networked MG-aided approach can improve the service restoration capability of a distribution grid. Future work includes the edition of wind energy, electric vehicles with demand response, and implementation on a real system.

6. References

[1] Campbell, R. J.: 'Weather-related power outages and electric system resiliency' (Library of Congress, 2012)

[2] Executive office of the President: ‚Economic benefits of increasing electric grid resilience to weather outages' (White House, 2013)

[3] Wei, Y., Ji, C., Galvan, F., Couvillon, S., Orellana, G.: 'Dynamic modeling and resilience for power distribution'. Proc. Int. Conf. Smart Grid Commun., 2013, pp. 85-90

[4] Che, L., Khodayar, M., Shahidehpour, M.: 'Only connect: Microgrids for distribution system restoration', IEEE Power Energy Mag., 2014 **12**, (1), pp. 70-81

[5] Wang, Z., Chen, B., Wang, J., Kim, J., Begovic, M. M.: 'Robust optimization based optimal DG placement in microgrids', *IEEE Trans. Smart Grid*, 2014, **5**, (5), pp. 2173-2182

[6] Moreira, C. L., Resende, F. O., Lopes, J. A. P.: 'Using low voltage MicroGrids for service restoration', *IEEE Trans. Power Syst.*, 2007, **22**, (1), pp. 395-403

[7] Wang, Z., Chen, B., Wang, J., Kim, J.: 'Decentralized energy management system for networked microgrids in grid-connected and islanded modes', *IEEE Trans. Smart Grid*, 2015, **7**, (2), pp. 1097-1105

[8] Wang, Z., Chen, B., Wang, J., Chen, C.: 'Networked microgrids for self-healing power systems', *IEEE Trans. Smart Grid*, 2016, **7**, (1), pp. 310-319

[9] Wang, Y., Chen, C., Wang, J., Baldick, R.: 'Research on resilience of power systems under natural disasters - a review', *IEEE Trans. Power Syst.*, 2016, **31**, (2), pp. 1604-1613

[10] Xu, Y., Liu, C. C., Schneider, K., Tuffner, F., Ton, D.: 'Microgrids for service restoration to critical load in a resilient distribution system', *IEEE Trans. Smart Grid*, accepted for publication

[11] Wang Z., Wang, J.: 'Self-healing resilient distribution systems based on sectionlization into microgrids', *IEEE Trans. Power Syst.*, 2015, **30**, (6), pp. 3139-3149

[12] Shahnia, F., Bourbour, S., Ghosh, A.: 'Coupling neighboring microgrids for overload management based on dynamic multicriteria decision making', *IEEE Trans. Smart Grid*, 2015, **8**, (2), pp. 969-983

[13] Li, J., Ma, X. Y., Liu, C. C., Schneider, K. P.: 'Distribution system restoration with microgrids using spanning tree search', *IEEE Trans. Power Syst.*, 2014, **29**, (6), pp. 3021-3029

[14] Siddiqui S., Gabriel, S. A.: 'An SOS1-based approach for solving MPECs with a natural gas market application', *Networks Spat. Econ.*, **13**, (2), 2012, pp. 205-227

[15] Torquato, R., Shi, Q., Xu, W., Freitas, W.: 'A monte carlo simulation platform for studying low voltage residential networks', *IEEE Trans. on Smart Grid*, 2014, **5**, (6), pp. 2766-2776

[16] Lu, N., Diao, R., Hafen, R., Samaan, N., Makarov, Y.: 'A comparison of forecast error generators for modeling wind and load uncertainty'. IEEE PES General Meeting, 2013, pp. 1-5

[17] Baran, M., Wu, F.: 'Optimal capacitor placement on radial distribution systems', *IEEE Trans. Power Del.*, 1989, **4**, (1), pp. 725-734

[18] Arif, A., Wang, Z., Wang, J., Chen, C.: 'Power distribution system outage management with co-optimization of repairs, reconfiguration, and DG dispatch', *IEEE Trans. on Smart Grid*, accepted for publication.

[19] Moshi, G. G., Bovo, C., Berizzi, A., Milano, P.: 'Optimal operational planning for PV-wind-diesel-battery microgrid'. Proc. IEEE PowerTech, 2015, pp. 1-6

[20] Jabr, R. A., Singh, R., Pal, B. C.: 'Minimum loss network reconfiguration using mixed-integer convex programming', *IEEE Trans. Power Syst.*, 2012, **27**, (2), pp. 1106-1116

[21] Bizuayehu, A. W., SÃ¡nchez de la Nieta, A. A., Contreras, J., CatalÃ£o, J. P. S.: 'Impacts of stochastic wind power and storage participation on economic dispatch in distribution systems', *IEEE Trans. on Sustain. Energy*, 2016, **7**, (3), pp. 1336-1345

[22] Hatziargyriou, N., Dimeas, A., Tsikalakis, A.: 'Centralized and decentralized control of microgrids', *Int. J. of Distrib. Energy Resources*, 2005, **1**, (3), pp. 197-212

[23] Shi, W., Xie, X., Chu, C. C., Gadh, R.: 'Distributed optimal energy management in microgrids', *IEEE Trans. Smart Grid*, 2015, **6**, (3), pp. 1137-1146

[24] Kim, H.M., Kinoshita, T., Shin, M.C.: 'A multiagent system for autonomous operation of islanded microgrids based on a power market environment', *Energies*, 2010, **3**, (12), pp. 1972-1990

[25] Kersting, W.: 'Radial distribution test feeders', *IEEE Trans. Power Syst.*, 1991, **6**, (3), pp. 975-985